31st Annual International Conference of the IEEE EMBS
Minneapolis, Minnesota, USA, September 2-6, 2009

Modeling Current Pathways for Therapeutic Electrical Applications

Robert Patterson, *Life Senior Member IEEE* and Fei Yang

Abstract—**In determining how various devices will provide therapeutic currents it is necessary to know the current pathways along with the current densities and voltage gradients in the tissues of interest and in other tissues that may be influenced. In order to obtain this information a high resolution, computer based model (3.8 million elements) was created using gated ECG MRI images from an adult male. The model used the finite difference approach to obtain the needed data. A user friendly, graphical interface was developed for a PC program. The features of the program along with examples from studying the electrical therapies of pacing and defibrillation will be given. It will be show that the conductivity of the entire thorax is important in determining the current pathways within the heart.**

I. INTRODUCTION

In treating various medical conditions with electrical current, it is desirable to know the exact current flow and current density in the tissues. It is important to know not only the current in the tissue of interest, but also the current in other tissues that could be at undesirable levels. Because it is very difficult to determine direct measurements of either the current pathways or current density, models are employed to obtain this information. In our laboratory, over many years, we have developed thoracic models to study current density, and voltage gradients throughout the chest using the finite difference method (FDM)[1]-[4]. The very early models were small (2500 elements) and were based on anatomy pictures in books. More recent models are based on gated MRIs and range from 216,000 to 3.8 million elements. We have also developed software to measure transfer impedance and sensitivity analysis to determine the contribution of various regions to the total impedance measured. The most recent version of the program has a very user friendly, graphical interface which runs on a PC.

We have used this model to determine how changes in the coil position in the ventricle influences current densities in the myocardium and throughout the chest [5]. Another study involved determining how pulmonary edema can change the threshold of implantable cardioverter defibrillators (ICD) due to changes in the distribution of currents in the thorax [6]. Lung edema changes the current distribution in the thorax resulting in higher defibrillation thresholds.

This presentation will trace the model development. It will present special features that make for easy use and also compare visual images of current density and voltage gradient fields for different resolution models. Data from the ICD studies will also be shown.

II. MEHTODS

A. Electrical thoracic modeling

The subject imaged as the anatomical source for our model was a 63 years old male, 100kg, 180cm in height. The MRI was performed with a 1.5 T Siemens Sonata instrument. Forty three thoracic transverse images were obtained from the abdomen to the neck. Images gated from the ECG were obtained every 50 ms over the cardiac cycle. To date only peak systole and diastole have been segmented and incorporated into the model. The images were digitized at a spatial resolution of 1.5 mm/pixel in right-left and anterior-posterior directions. The resolution in the cranial-caudal direction was 5 mm/pixel equal to the MRI slice thickness. Each tissue was assigned an appropriate electrical resistivity. A 3D diastolic ECG-gated electrical model of the thorax was thus created, with 3.8 million elements and 1.5x1.5x5 mm resolution. The validity of the model has been established by many studies.

B. Problem formulation

The model was developed using the finite difference method (FDM). Only the basic formulations of FDM is given below

The Poisson's equation (1), the governing equations of the problem, can be rewritten as

$$\nabla \sigma \nabla V + F = 0 \qquad (1)$$

in which the conductivity σ, the reciprocal of ρ, is used to simplify the expressions. By using FDM, it can be solved numerically, to obtain discrete values at certain locations (nodes).

C. Numerical solution

To solve (1) using FDM, first the calculation domain is divided into a number of non-overlapping control volumes (CV) such that there is one CV surrounding each grid point or node indicated by capital letters W, P, E, S, N, U, and L, as shown in Fig. 1. These grid points or nodes correspond to the grid points in the 3D thoracic model. Next

Manuscript received April 7, 2009.

R. P. Patterson is with the University of Minnesota, 420 Delaware St., MMC 297, Minneapolis MN 55455 (corresponding author phone: 612-626-3308; e-mail: patte001@umn.edu).

F. Yang. was with University of Minnesota, Minneapolis, MN 55455 USA.

the control volume around the grid point P is used as an example. The grid point P has W (as west), E (as east), S (south), N (north), U (as upper) and L (as lower) as its neighbors.

In Fig. 1, control volume (CV) and the CV faces are indicated by e and w in x direction, s and n in y direction, and u and l in z direction. Δx, Δy, *and* Δz are the distances between the CV faces in *x*, *y* and *z* directions. $(\delta x)_w$ and $(\delta x)_e$, $(\delta y)_s$ and $(\delta y)_n$, $(\delta z)_u$ and $(\delta z)_l$ are distances between nodes W and P, P and E, S and P, P and N, U and P, and P and L in *x*, *y* and *z* directions. σ_e, σ_w, σ_s, σ_n, σ_u, and σ_l are conductivities at CV faces *w* and *e*, *s* and *n*, and *u* and *l*. $\bar{F}$ is the average current source value over the CV.

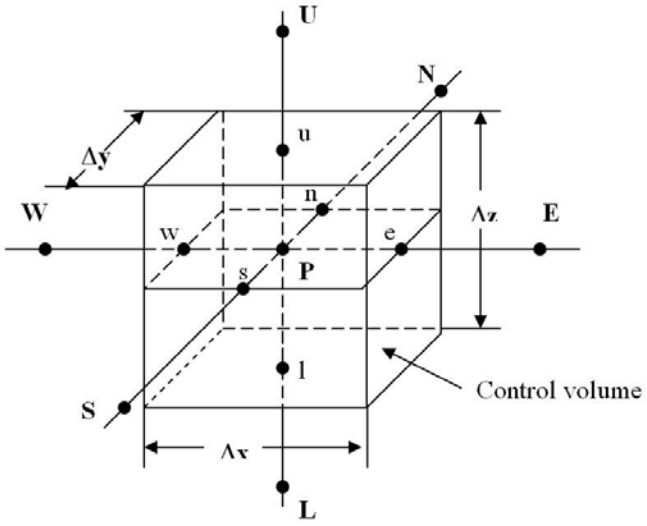

Fig. 1 3D Control volume surrounding grid point P

It can be derived that the discrete equation for node P is

$$a_P V_P = a_E V_E + a_W V_W + a_N V_N + a_S V_S + a_U V_U + a_L V_L + b$$

where:

$$a_E = \frac{\sigma_e}{(\delta x)_e}\Delta y \Delta z, \qquad a_W = \frac{\sigma_w}{(\delta x)_w}\Delta y \Delta z$$

$$a_N = \frac{\sigma_n}{(\delta y)_n}\Delta x \Delta z, \qquad a_S = \frac{\sigma_s}{(\delta y)_s}\Delta x \Delta z$$

$$a_U = \frac{\sigma_u}{(\delta z)_u}\Delta x \Delta y, \qquad a_L = \frac{\sigma_l}{(\delta z)_l}\Delta x \Delta y$$

$$a_P = a_E + a_W + a_N + a_S + a_U + a_L$$

$$b = \bar{F}\,\Delta x \Delta y \Delta z$$

The above equations were coded efficiently in C++. Recently a very user friendly graphical interface was developed as a tool box for Matlab. This is referred to as ZMIND

Below is a screen capture shot of the interface screen. The users can select an axial view of each of 43 slices. Also views in the coronal and sagittal plane can be shown.

View 1 shows an axial image of the tissue types shown by color. View 2 shows an axial view of the tissue resistivity with the colors indicating the values. View 3 shows the potential by color and electrical field with arrows indicating the voltage gradient direction and strength. View 4 shows an axial view of the current density. The program can also calculate four electrode impedance values and sensitivity through out the volume. These results are shown in the space below the images.

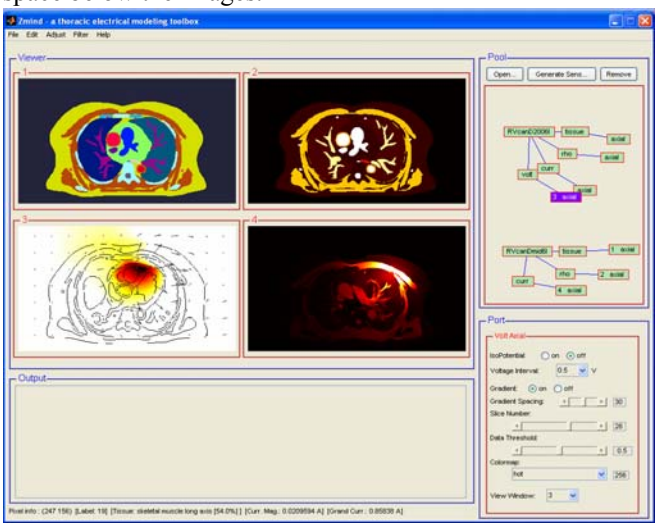

Fig. 2 A screen shot from ZMIND

III. Results

The comparison of the current density pattern for similar current excitations is shown below for a model with 216,000 elements and one with 2.8 million elements.

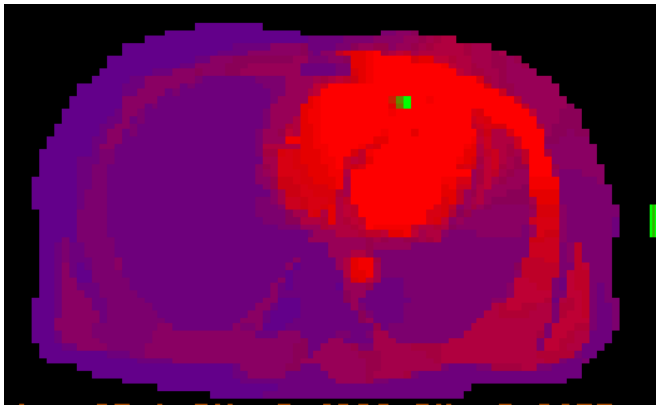

Figure 3 Current density for a model with 216,000 elements with pixel dimensions of 10x3.7x4.2 mm

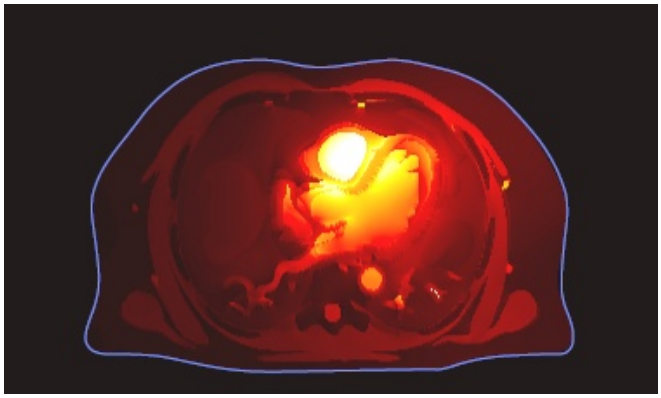

Fig. 4 Current density for a model with 3.8 million elements with pixel dimensions of 5x1.5x1.5 mm

The program can display axial, coronal, and sagittal views for both the current density and voltage with gradients. Fig. 5 is a coronal voltage map with gradients. Because the thickness of the MRI slices are 5 mm the resolution is poorer compared to the axial views.

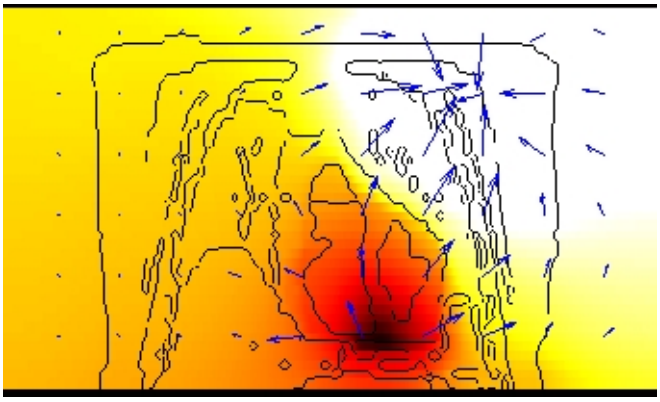

Fig. 5 Coronal view of voltage gradients for cardiac pacing

Fig. 6 and 7 depict the change in current densities as a result of pacing between the right ventricle and can. The mid-thorax axial images as a function of lung resistivity, in which the lung resistivity was changed from 1400 ohm-cm to 400 ohm-cm are shown in Fig. 6 and 7 respectively. When the lung resistivity is normal more current is flowing in the skeletal muscle, great vessels and myocardium compared to the case with lower lung resistivity. As a result of this the defibrillation threshold increases i.e. more current is needed [6].

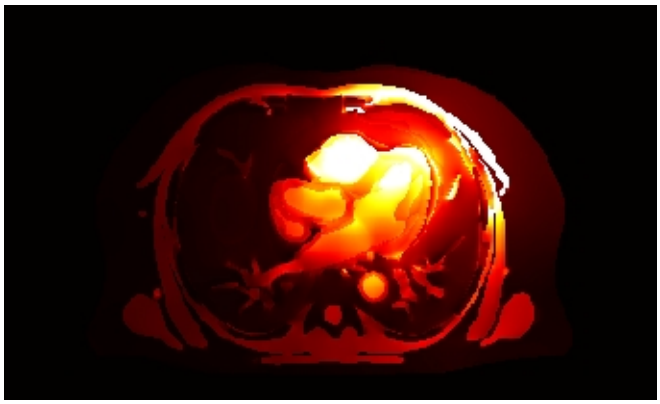

Fig 6. Current density during pacing between the RV and can with normal lung resistivity of 1400 ohm-cm.

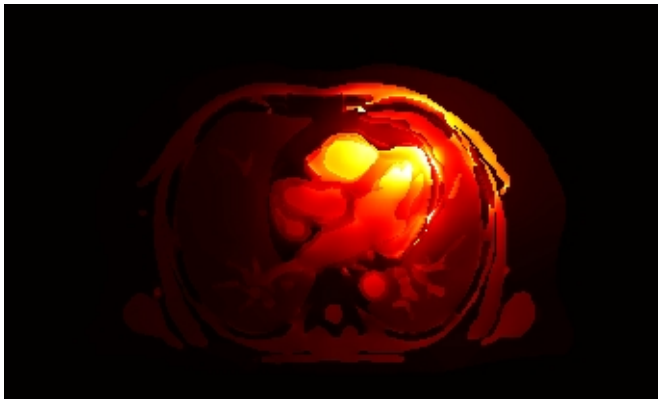

Fig 7. Current density during pacing between the RV and can with edematous lung resistivity of 400 ohm-cm.

IV. Conclusion

The package of a set of MRIs from tissues of interest along with user friendly software allows one to carefully determine where the current flows. The examples shown above demonstrate that in the case of the heart one cannot assume that the other tissues in the thorax do not influence the current pathway. Our previously published study [6] showed that lung edema resulted in an increase in defibrillator thresholds.

Acknowledgment

We would like to thank the Minnesota Supercomputing Institute for computation resources.

References

[1] R.P.Patterson, "Sources of the thoracic cardiogenic electrical impedance signal as determined by a model". *Med. Biol. Eng. Comput.*Vol. 23, pp. 411-417, 1985.

[2] L. Wang, R. Patterson, "Multiple sources of the impedance cardiogram based on 3D finite difference human thorax models". *IEEE Trans on Biomed. Eng*. Vol 42, pp. 393-400, 1995.

[3] A. Belalcazar., R. P. Patterson, "Improved lung edema monitoring with coronary vein pacing leads: a simulation study". *Physiol. Meas*. Vol. 25 pp. 475-487, 2004.

[4] F. Yang, R. Patterson, "The contribution of the lungs to thoracic impedance measurements: a simulation study based on a high resolution finite difference model", *Physiol. Meas.* Vol. 28, pp. s153-s163, 2007.

[5] F. Yang and R. Patterson " Optimal transvenous coil position on active-can single-coil ICD defibrillation efficacy: a simulation study" *Annals of Biomedical Engineering,* vol. 36, pp. 1659-67, 2008.

[6} F. Yang and R. P. Patterson , "Effect of cardiogenic pulmonary edema on defibrillation efficacy", *International Journal of Cardiology* xx (2009) xxx–xxx (On the Internet with print version to follow).